Title: A calcium-dependent pathway underlies activity-dependent plasticity of electrical synapses in the thalamic reticular nucleus

Authors: Jessica Sevetson, Sarah Fittro, Emily Heckman and Julie S. Haas*

Department of Biological Sciences

Lehigh University

111 Research Drive, Bethlehem, PA 18015.

*correspondence: julie.haas@lehigh.edu

Figures: 8

Keywords: gap junction connexin36 LTD

Additional Information:

No **competing interests** are declared.

Author contributions: JSH conceived and designed the experiments. JS, SF, EH and JSH collected, analyzed and interpreted data. JS and JSH drafted and revised the manuscript.

Funding: JSH was supported by the Brain & Behavior Research Foundation (Haddie Investigator), the Whitehall Foundation, and NSF IOS 1557474

Acknowledgements: The authors thank Bruce Bean (Harvard University) for providing TTA-A2 and Aniruddha Ghosh for help in data collection.

All authors approved submission of this version of the manuscript.

Key Points Summary:

- Electrical synapses are modified by various forms of activity, including paired activity in coupled neurons and tetanization of the input to coupled neurons.
- We show that plasticity of electrical synapses that results from paired spiking activity in coupled neurons depends on calcium influx and calcium-initiated signaling pathways.
- Plasticity that results from tetanization of input fibers does not depend on calcium influx or dynamics.
- These results imply that electrically coupled neurons have distinct sets of mechanisms for adjusting coupling according to the specific type of activity they experience.

Abstract

Recent results have demonstrated modification of electrical synapse strength by varied forms of neuronal activity. However, the mechanisms underlying plasticity induction in central mammalian neurons are unclear. Here we show that the two established inductors of plasticity at electrical synapses in the thalamic reticular nucleus -- paired burst spiking in coupled neurons, and mGluR-dependent tetanization of synaptic input -- are separate pathways that converge at a common downstream endpoint. Using occlusion experiments and pharmacology in patched pairs of coupled neurons in vitro, we show that burst-induced depression depends on calcium entry via voltage-gated channels, is blocked by BAPTA chelation, and recruits intracellular calcium release on its way to activation of phosphatase activity. In contrast, mGluR-dependent plasticity is independent of calcium entry or calcium dynamics. Together, these results show that the spiking-initiated mechanisms underlying electrical synapse plasticity are similar to those that induce plasticity at chemical synapses, and offer the possibility that calcium-regulated mechanisms may also lead to alternate outcomes, such as potentiation. Because these mechanistic elements are widely found in mature neurons, we expect them to apply broadly to electrical synapses across the brain, acting as the crucial link between neuronal activity and electrical synapse strength.

Abbreviations:

TRN, thalamic reticular nucleus; LTD, long-term depression; mGluR, metabotropic glutamate receptor; ACPD, (±)-1-Aminocyclopentane-trans-1,3-dicarboxylic acid; Cx36, connexin36

Introduction

The thalamic reticular nucleus (TRN) is a brain area crucial for generation of sleep spindle rhythms (Steriade *et al.*, 1987) and is thought to focus the cortical 'searchlight' of attention (Crick, 1984; McAlonan *et al.*, 2006). This central brain nucleus functions as a gate for the bidirectional flow of activity and information between the thalamus and the cortex, receiving its major source of excitatory input from topographically organized as well as diffuse crossmodal collaterals of both thalamocortical and corticothalamic axons. The synaptic targets of inhibition from the TRN are the thalamic relay neurons (Ohara & Lieberman, 1985; Pinault & Deschenes, 1998). Within the TRN, connexin36-based electrical synapses are the main substrate for neuronal communication (Landisman *et al.*, 2002). Thus, the electrical synapses in the TRN, and their strength, are likely key regulators of brain rhythms and attention.

At present, two types of activity are known to induce plasticity at electrical synapses of the TRN. The first induction pattern is through paired bursts of spiking activity in coupled neurons. Burst firing in TRN is a prominent component of both sleep spindle rhythms and the sharp wave discharges that characterize *absence* seizures (Inoue *et al.*, 1993; von Krosigk *et al.*, 1993; Huguenard & Prince, 1994; Destexhe, 1998; Steriade, 2005). When two electrically coupled TRN neurons are made to fire synchronized bursts, the electrical synapse connecting them undergoes long-term depression (LTD)(Haas *et al.*, 2011).

The second established paradigm for inducing plasticity is tetanization of afferent cortical input to coupled TRN neurons, which leads to LTD that is mediated by the recipient metabotropic glutamate receptors (mGluRs) (Landisman & Connors, 2005). In mGluR-dependent LTD, induced by bath application of the agonist ACPD, group I and group II mGluRs modulate coupling through opposing effects: activation of group I mGluRs works through a Gs

signaling pathway, stimulating adenylyl cyclase, activating PKA and resulting in depression, while activation of the group II receptor mGluR3 yields potentiation through activation of Gi/o, adenylyl cyclase and inhibition of PKA (Wang *et al.*, 2015).

Diverse and critical roles for calcium in synaptic plasticity have been widely characterized in chemical synapses. In many instances, LTP arises from protein kinase activity, where LTD results from protein phosphatase activity (Collingridge *et al.*; Malenka & Bear, 2004; Xia & Storm, 2005). For electrical synapses, there are preliminary indications for calcium entry as a mediator for expression of plasticity. At the goldfish Mauthner mixed glutamatergic-electrical synapse, considerable evidence shows that calcium influx through NMDA receptors leads to increases in strength in both the chemical and electrical components of the mixed synapse mediated by CaMKII (Pereda & Faber, 1996; Cachope & Pereda, 2012). In the retina, nonsynaptic NMDA receptors mediate activity-dependent plasticity of coupling in the AII amacrine cell network (Kothmann *et al.*, 2012). Long-lasting depression of electrical synapses between pairs of inferior olivary cells results from 1-Hz stimulation of adjacent white matter, and this effect is NMDA-dependent (Mathy *et al.*, 2014), while higher-frequency stimulation or NMDA application potentiates coupling (Turecek *et al.*, 2014).

We explored whether burst-induced LTD and mGluR-dependent LTD share a calcium-mediated mechanism. Our results demonstrate that while burst-induced and ACPD-induced mGluR-dependent LTD of electrical synapses occlude each other, the burst-induced form of plasticity depends on calcium influx through voltage-gated channels that leads to intracellular calcium release and phosphatase activation, while the ACPD-induced plasticity is independent of calcium influx. Together, these results demonstrate that electrical synapse strength changes independently and specifically to incoming and intrinsic forms of neuronal activity. Additionally,

the calcium dependence of burst-induced plasticity suggests the possibility for bidirectional regulation of electrical synapse strength similar to that found at neurotransmitter-based synapses.

Methods

Electrophysiology Horizontal slices 350-400 µm thick were obtained from Sprague-Dawley rats aged P11 - P14 of both sexes, in accordance with previous studies in TRN (Haas et al., 2011). Rats were anesthetized by inhaled isofluorane (5 mL of isoflurane applied to fabric, within a 1 L chamber) and euthanized by decapitation, in accordance with federal and Lehigh University IACUC animal welfare guidelines. Slices were cut and incubated in sucrose solution (in mM): 72 sucrose, 83 NaCl, 2.5 KCl, 1 NaPO₄, 3.3 MgSO₄, 26.2 NaHCO₃, 22 dextrose, 0.5 CaCl₂. Slices were incubated at 37°C for 20 min and returned to room temperature until recording. The bath for solution during recording contained (in mM): 126 NaCl, 3 KCl, 1.25 NaH₂PO₄, 2 MgSO₄, 26 NaHCO₃, 10 dextrose and 2 CaCl₂, 300-305 mOsm, saturated with 95% O₂/ 5% CO₂. The submersion recording chamber was held at 34°C (TC-324B, Warner Instruments). Micropipettes were filled with (in mM): 135 K-gluconate, 2 KCl, 4 NaCl, 10 HEPES, 0.2 EGTA, 4 ATP-Mg, 0.3 GTP-Tris, and 10 phosphocreatine-Tris (pH 7.25, 295 mOsm). 1M KOH was used to adjust pH of the internal solution. The approximate bath flow rate was 2 ml/min and the recording chamber held approximately 5 ml solution. The specific T-channel antagonist TTA-A2 was generously provided by Dr. Bruce Bean (Harvard University) and made into stock aliquots of 3 mM, in DMSO. Other drugs applied, including (\pm) -1-Aminocyclopentane-trans-1,3-dicarboxylic

acid (ACPD); 1,2-Bis(2-aminophenoxy)ethane-N,N,N',N'-tetraacetic acid (BAPTA); nimodipine, caffeine,(-)- xestospongin-C, FK 506, and cyclosporin-A (acquired as 1 mg/ml solution in DMSO) were acquired from Tocris or Sigma, and diluted into high-concentration stock solutions in DMSO or water before final dilution. Final DMSO concentration was always < 0.2%. Caffeine was dissolved in ACSF buffered for pH with HEPES. Drugs were bath-applied continuously unless noted otherwise.

The TRN was visualized under 5x, and pairs of TRN cells were identified with 40x IR-DIC optics (SliceScope, Scientifica). Signals were amplified and low-pass filtered at 8 kHz (MultiClamp, Axon Instruments), digitized at 20 kHz (lab-written Matlab routines controlling a National Instruments USB6221 DAQ board), and stored for offline analysis in Matlab (Mathworks, R2012a). All recordings were made in whole-cell current-clamp mode. Values of V_{rest} ranged from -50 to -70 mV, and negative current was used to maintain all cells at -70 mV during measurement of coupling in order to accurately measure it (Curti & Pereda, 2004; Curti *et al.*, 2012; Haas & Landisman, 2012b). Pipette resistances were 4-8 M Ω before bridge balance, which was discarded if it exceeded 25 M Ω . Voltages are reported uncorrected for the liquid junction potential. During ACPD application, further negative current was added to prevent spiking that could become bursting and confound the induction stimuli we sought to separate, but neurons were allowed to depolarize to just below threshold. Paired bursting was induced by current injection through the recording electrodes for 50 ms at 2 Hz, as described in Haas et al. 2011.

Numerical analysis Input resistances for each cell and coupling between cells were quantified by injecting 100 pA of hyperpolarizing current into one cell of a coupled pair, and measuring

voltage deflections in that cell (ΔV) and in the coupled neighbor (δV). The coupling coefficient cc is computed as $\delta V/\Delta V$. Coupling coefficients reported here are averaged over 10 measurements in both directions. Coupling conductance G_c was estimated separately for each direction (Fortier, 2010; Sevetson & Haas, 2015), and averaged over both directions. For plasticity experiments, experiments were discarded when R_{in} of either cell in a pair deviated by more than 20% from initial values. Changes in coupling were evaluated as the average over the first 20 min following activity or ACPD, compared to normalized baseline values, and are reported as mean \pm SEM. We report t-tests as two-tailed paired comparisons of pre- and post-stimulus averages unless stated otherwise, and report the results as as p_t . Two-sided Wilcoxon signed rank tests were also carried out on the sets of change in coupling for each condition, and are reported as p_s . No multiple comparisons were performed.

Results

Although LTD of electrical synapses has been induced both by paired bursting activity in coupled cells and by pharmacological tetanization of mGluRs by ACPD, it was unknown how these two types of LTD are related, or whether these two paradigms share common downstream molecular mechanisms. To explore the possibility of common mechanisms, we induced LTD in pairs of coupled TRN neurons with one paradigm and followed it with the other. We induced LTD using paired bursting, resulting in LTD of coupling conductance and coefficient (Fig. 1A-D; $\Delta G_C = -11.6 \pm 1.0\%$, $p_t = 0.003$, $p_s = 0.008$; $\Delta cc = -11.8 \pm 1.3\%$, $p_t = 0.002$, $p_s = 0.008$; n = 8 pairs). After ten minutes of measuring post-burst LTD, we bath-applied ACPD (50 μ M) for 4 minutes. Following ACPD application, we saw no further significant changes in electrical

synapse strength ($p_t = 0.58$, $p_s = 0.95$; $p_t = 0.66$ and $p_s = 0.74$ for comparison between post-burst and post-ACPD values of ΔG_C and cc, respectively). In a separate set of experiments, we first induced depression with 3-4 min of ACPD, which depressed mean coupling conductance (Fig. 2 F-I; $\Delta G_C = -8.6 \pm 0.9\%$, $p_t = 0.0001$, $p_s = 0.008$; $\Delta cc = -8.2 \pm 0.9\%$, $p_t = 0.01$, $p_s = 0.02$; n = 8 pairs). Ten minutes after ACPD washout, we induced paired bursting. Following paired activity, mean coupling conductance and coupling coefficient remained depressed without further change ($p_t = 0.22$, $p_s = 0.15$; $p_t = 0.35$ and $p_s = 0.55$ for the comparison between post-ACPD and post-burst values of ΔG_C and cc, respectively). These experiments demonstrate that for both types of plasticity, induction of LTD via one paradigm occluded the depression previously observed following the other plasticity paradigm and indicate that both burst-induced and ACPD-induced plasticity share a common downstream mechanism for depressing electrical synapses.

Similar to most thalamic neurons, in neurons of the TRN the Cav3.2 T-type calcium currents are a dominant influence on spiking and source of calcium influx (Huguenard & Prince, 1992; Talley *et al.*, 1999). To determine a role for this major calcium current in electrical synapse plasticity in the TRN, we examined its influence on both forms of plasticity with the potent, specific antagonist TTA-A2 (1 μ M)(Kraus *et al.*, 2010). Paired bursting in TTA-A2 failed to induce changes in electrical synapse strength (Fig. 2A-D; $\Delta G_C = -1.2 \pm 1.0\%$, $p_t = 0.9$, $p_s = 0.77$; $\Delta cc = -1.4 \pm 1.5\%$, p = 0.8, $p_s = 1$; p = 10 pairs). Bath application of ACPD in the presence of TTA-A2, however, still resulted in depression (Fig. 2F-J; $\Delta G_C = -12.0 \pm 1.5\%$, $p_t = 0.002$, $p_s = 0.008$; $\Delta cc = -11.0 \pm 1.5\%$, $p_t = 0.001$, $p_s = 0.008$; $p_t = 0.008$

in normal ACSF and burst-induced changes in nimodipine was not significant (unpaired t-test, p = 0.54), implying that T-type, and not L-type, channels are the main source of calcium that drives plasticity of electrical synapses in the TRN. Together, these results indicate that the bursting activity-induced form of LTD depends on calcium influx through voltage-gated channels, primarily T channels, while the afferent ACPD-induced plasticity does not.

Next, we verified a role for the increase in intracellular calcium concentration in inducing plasticity of electrical synapses by chelating calcium with BAPTA (10 mM) in the intracellular solution. Synchronous bursting in pairs of coupled neurons that included BAPTA resulted in no change in electrical synapse strength (Fig. 4 A-D; $\Delta G_C = 1.67 \pm 1.2\%$, $p_t = 0.28$, $p_s = 0.47$ and $\Delta cc = -0.34 \pm 0.9\%$, $p_t = 0.71$, $p_s = 0.85$, n = 12 pairs), confirming the dynamic role of calcium after its influx through T-type channels during paired bursting in inducing LTD. In contrast, ACPD application to pairs of coupled neurons in BAPTA did depress the synapse (Fig. 4 F-I; $\Delta G_C = -12.0 \pm 1.2\%$, $p_t = 0.026$, $p_s = 0.015$ and $\Delta cc = -8.9 \pm 1.2\%$, $p_t = 4.4 \times 10^{-6}$, $p_s = 0.014$; n = 8 pairs), also confirming that calcium flux across and within the membrane is not required for ACPD-induced LTD.

Calcium influx often induces release of calcium (calcium induced calcium release, or CICR) from stores within the endoplasmic reticulum, via either ryanodine-sensitive or IP₃ – sensitive receptors, which is a common component in chemical synaptic plasticity pathways (Svoboda & Mainen, 1999). In TRN, ryanodine receptors have been shown to contribute to the spiking pattern of bursts (Coulon *et al.*, 2009), and IP₃-mediated calcium release has also been shown (Neyer *et al.*, 2016). We examined the role of CICR through both types of receptors for burst-induced plasticity. Because our results in BAPTA showed that ACPD-induced LTD occurred independently of calcium influx (although a 4x-higher concentration, 200 μM ACPD,

has been shown to result in calcium release (Never et al., 2016)), we did not pursue further calcium-related mechanisms for that inductor. We used caffeine (5 mM) to extinguish ryanodinesensitive stores. Paired bursting in caffeine did not change coupling conductance (Fig. 5 A-D; $\Delta G_C = 6.7 \pm 1.4\%$, $p_t = 0.31$, $p_s = 0.41$; n = 11 pairs), although lowered input resistance (Fig. 5E; $\Delta R_{in} = -11.7 \pm 1.6\%$, p = 0.007), possibly arising from nonspecific effects of caffeine on voltagedependent membrane conductances, resulted in a slightly lower mean coupling coefficient (Δcc = -5.7 \pm 1.0%, p_t = 0.09, p_s = 0.31; n = 11 pairs). Caffeine application alone (with no activity), used to release calcium from ryanodine-sensitive stores, had no effect on baseline electrical synapse strength (not shown; $\Delta G_C = 1.8 \pm 1.6\%$; $\Delta cc = 3.5 \pm 1.6\%$, n= 7 pairs, p > 0.05). To further clarify the role of ryanodine-sensitive calcium release, we repeated experiments with ryanodine (10 µM in the internal solution (Carter et al., 2002)) which also blocked LTD, though some rundown was observed (Fig. 5F-I; for t < 15 min, $\Delta G_C = 0.88 \pm 1.8\%$, $p_t = 0.6$, $p_s = 0.6$; $\Delta cc = -2.1 \pm 1.9\%$, $p_t = 0.07$, $p_s = 0.32$; n = 11 pairs). Turning to IP₃-mediated release, we antagonized IP₃ receptors with the specific antagonist xestospongin-C (1 µM) (Gafni et al., 1997), and in this condition, paired bursting resulted in LTD that was not significant over the pairs tested (Fig. 6 A-D; $\Delta G_C = -6.0 \pm 1.1\%$, $p_t = 0.16$, $p_s = 0.11$; $\Delta cc = -12.4 \pm 1.1\%$, $p_t = 0.093$, $p_s = 0.08$; n = 9 pairs). Together, this set of results indicate that CICR is a contributor to burstinduced plasticity at electrical synapses.

Finally, we tested a possible target of intracellular calcium that could interact with the known phosphorylation sites of Cx36. In addition to the PKA-mediated depression already described (Wang *et al.*, 2015), several studies have demonstrated increases of Cx36-based electrical coupling or of its ortholog Cx35 at known phosphorylation sites via cAMP and PKA (Mitropoulou & Bruzzone, 2003), or through Ca²⁺/CaMKII signaling pathways (Alev *et al.*,

2008) (Del Corsso *et al.*, 2012). To test the hypothesis that LTD might arise from dephosphorylation, we used FK-506 (1 μ M) to inhibit the calcium-activated protein phosphatase 2B calcineurin (Liu *et al.*, 1991). In FK-506, paired bursting failed to depress the synapse (Fig. 7 A-D; $\Delta G_C = -4.1 \pm 1.0\%$, $p_t = 0.91$, $p_s = 0.37$; $\Delta c_c = -3.1 \pm 0.9\%$, $p_t = 0.28$, $p_s = 0.41$; n = 9 pairs). Because FK-506 may interact with neuronal ryanodine receptors (Gant *et al.*, 2014), we also repeated paired bursts with the calcineurin inhibitor cyclosporin A (1 μ M in the internal solution (Li *et al.*, 2003)). With cyclosporin A, paired bursting still failed to depress the synapses (Fig. 7 F-I; $\Delta G_C = 0.04 \pm 1.5\%$, $p_t = 0.36$, $p_s = 0.81$; $\Delta c_c = -2.5 \pm 1.6\%$, $p_t = 0.38$, $p_s = 0.58$; n = 7 pairs), confirming the participation of calcineurin in LTD of electrical synapses. Thus, we conclude that calcium activation of the phosphatase calcineurin is necessary for bursting activity-induced LTD.

Our findings are summarized by the pathway in Figure 8. Briefly, we confirm that synchronous bursting and ACPD-induced activation of mGluR receptors are both inductors of plasticity of electrical synapses in TRN neurons. Our results here show that these inductors are separated by their dependence on calcium: bursting activity in TRN neurons drives calcium influx, mainly through T channels, that activates calcium release within the cell and ultimately activates a phosphatase that may dephosphorylates the Cx36 protein. In contrast, we show that the pharmacological activation of mGluRs to TRN by ACPD that has been shown to differentially drive an adenylyl cyclase/PKA-mediated pathway (Wang *et al.*, 2015) is independent of calcium entry and calcium flux.

Discussion

Together, our results support two major conclusions: first, that there are biochemically and physiologically separable forms of plasticity at electrical synapses, induced by different activity patterns and pathways but converging at the level of phosphorylation. The resulting plasticity is capable of exerting profound effects on the activity and synchrony of the coupled cells. Second, the involvement of calcium dynamics as a central element for burst-induced depression raises the possibility that a calcium influx- or calcium-dependent regulator that, for other types or conditions of calcium influx than used here, might lead to potentiation of the synapse.

Separable forms of plasticity. Our findings indicate that there are at least two independent forms of plasticity at electrical synapses. Importantly, these forms of plasticity are induced by different activity patterns and pathways – intrinsic and afferent activity -- that converge at the level of kinase/phosphatase activity on Cx36. These two forms render TRN neurons and synapses sensitive to varied types of activity, allowing synapses and synchrony to be modified specifically to precise forms of activity.

The mGluR-mediated LTD is more likely to be a broad phenomenon, affecting many neighboring electrical synapses in the TRN for the same bolus of glutamate released by presynaptic neurons. Because it depends on synaptic activation, it is a response to activity levels elsewhere in the brain. This form of LTD would then release many TRN neurons from their coupled neighbors' influences simultaneously, decreasing synchrony across a wide subsector of the TRN.

The burst-dependent form of LTD is initiated only by activity in pairs of coupled neurons, and is thus more sensitive to individual neuronal activity and acts on individual synapses. Regulation of this form of LTD by calcium implies that even the magnitude of the

plasticity at individual synapses is finely adjusted according to the precise amounts of activity at that particular synapse. Spiking in individual cells also likely relies on presynaptic activation to drive spiking, but at a cell-by-cell level.

Thus, two forms of electrical synapse LTD in the TRN give the nucleus finely sensitive ways to respond to the varied types of inputs (cortical, thalamic, and internal) it receives, and modulate its sensitivity and synchrony accordingly.

Convergence of the two forms would presumably allow the synapse to undergo plasticity for multiple reasons, but act as a way to limit plasticity from summing and driving large amounts of change in a short period of time. This finding also fits in with the common biological theme of the evolutionary advantage of having increased axes of control, especially for delicate or important processes. In other words, the fact that multiple pathways exist for inducing plasticity at an electrical synapse underlines their fundamental importance to the mammalian brain.

The Impact of Plasticity of Electrical Synapses. The speed and bidirectionality of electrical synaptic transmission allow coupled cells to rapidly share voltage deflections among coupled neighbors. Both subthreshold membrane fluctuations (Devor & Yarom, 2002; Long *et al.*, 2002; Beierlein *et al.*, 2003; Curti & Pereda, 2004; Long *et al.*, 2004; Haas & Landisman, 2012b) and action potentials (Galarreta & Hestrin, 2001), (Gibson *et al.*, 1999; Mann-Metzer & Yarom, 1999; Landisman *et al.*, 2002; Apostolides & Trussell, 2013) readily synchronize in many neuronal types, even with moderate electrical coupling strengths. As synapses go, electrical synapses are powerful physiological influences. We have shown that electrical synapses in TRN can directly evoke spikes in a neighbor (Haas & Landisman, 2012b, a), and results from electrically coupled neurons of the auditory brainstem show similar power (Apostolides &

Trussell, 2013, 2014). In TRN, we also showed that electrical synapses can accelerate spike times in neighbors by tens of ms, while the effects of an average glutamatergic excitatory synapse are limited to about a single ms (Sevetson & Haas, 2015).

ACPD-induced plasticity was previously shown to substantially desynchronize regular spiking in TRN neurons (Landisman & Connors, 2005). Burst-induced changes in electrical synapse strength that are small in absolute magnitude, ~15% (G_C or cc) are sufficient to silence a synapse, from one that induces spikes in neighbors, to an ineffective synapse (Haas *et al.*, 2011). Further, these numerically modest changes in synaptic strength yield 5-10 ms changes in spike times in coupled neighbors (Haas, 2015). Thus, even seemingly mild changes in electrical synapse strength produce physiologically substantial effects, and are poised to exert major influence on TRN synchrony and processing.

Calcium as a mediator of plasticity. Another major implication of our results is the involvement of spiking-related calcium influx and dynamics as a mediator for activity-induced depression. Calcium provides a direct link between spiking-related ion flow across a membrane, and synaptic strength. Further, the commonality with the many forms of calcium-dependent mechanisms of chemical synaptic plasticity indicate that these same mechanisms may be used, with variations, to adjust electrical synaptic strength all over the brain. Calcium dependence also suggests that other types or amounts of activity-related calcium influx might lead to potentiation of the synapse, similarly to rules shown for glutamatergic synapses (Dudek & Bear, 1992).

The mechanisms shown here could overlap with the indications for the established role of NMDA-mediated calcium influx in modifying electrical synapses shown in other systems through phosphorylation mechanisms. At the goldfish Mauthner club ending, where electrical

and glutamatergic synapses colocalize, calcium influx through nearby NMDA receptors during tetanizing stimuli is necessary for increases in both the chemical and electrical components of the mixed synapse (Yang *et al.*, 1990; Pereda & Faber, 1996; Cachope & Pereda, 2012) that are mediated by CAMKII (Pereda *et al.*, 1998). In retinal amacrine cells, glutamate spillover from bipolar cell activity activates NMDA receptors, and subsequently CaMKII, resulting in phosphorylation of Cx36 (Kothmann *et al.*, 2012) that potentiates electrical coupling. High-frequency stimulation or NMDA application potentiates coupling in the IO through CamKII (Turecek *et al.*, 2014), while long-lasting depression of electrical synapses between pairs of inferior olivary cells results from 1-Hz stimulation of adjacent white matter, in an NMDA-dependent effect (Mathy *et al.*, 2014).

Our report of a pathway between phosphatase activation and depression are consistent with previous reports, which overall indicate that kinase activation results in potentiation (Pereda et al., 1998; Cachope et al., 2007; Kothmann et al., 2012); (Turecek et al., 2014). Calciuminitiated kinase/phosphorylation pathways can potentially directly or indirectly target multiple phosphorylation sites on Cx36 (Kothmann et al., 2007; Alev et al., 2008). However, in the TRN, ACPD alters electrical synapses through a set of opposing effects: activation of group I mGluR receptors upregulates AC and eventually activates PKA, resulting in LTD; while activation group II mGluRs downregulates AC and inhibits PKA, resulting in potentiation (Wang et al., 2015). Together, these results and ours suggest that there are several possible phosphorylation-based mechanisms for regulating electrical synapse strength in TRN neurons. The relatively small magnitude of LTD of electrical synapses, combined with possible secondary effects of the calcium-interfering compounds used here, suggest that a note of caution should accompany these interpretations.

Despite the important role for calcium, it remains to be seen whether calcium flow across the gap junction is required for plasticity; focused imaging experiments may help elucidate this point. It also remains to be seen whether crosstalk, such as activation of adenylyl cyclase by calcineurin (Chan *et al.*, 2005), or parallel paths, such as calmodulin (Burr *et al.*, 2005), might exist among the pathways we have demonstrated. Nevertheless, determining the specifics of the role of calcium, its mediators and the resulting forms of plasticity will represent a worthwhile endeavor for future studies.

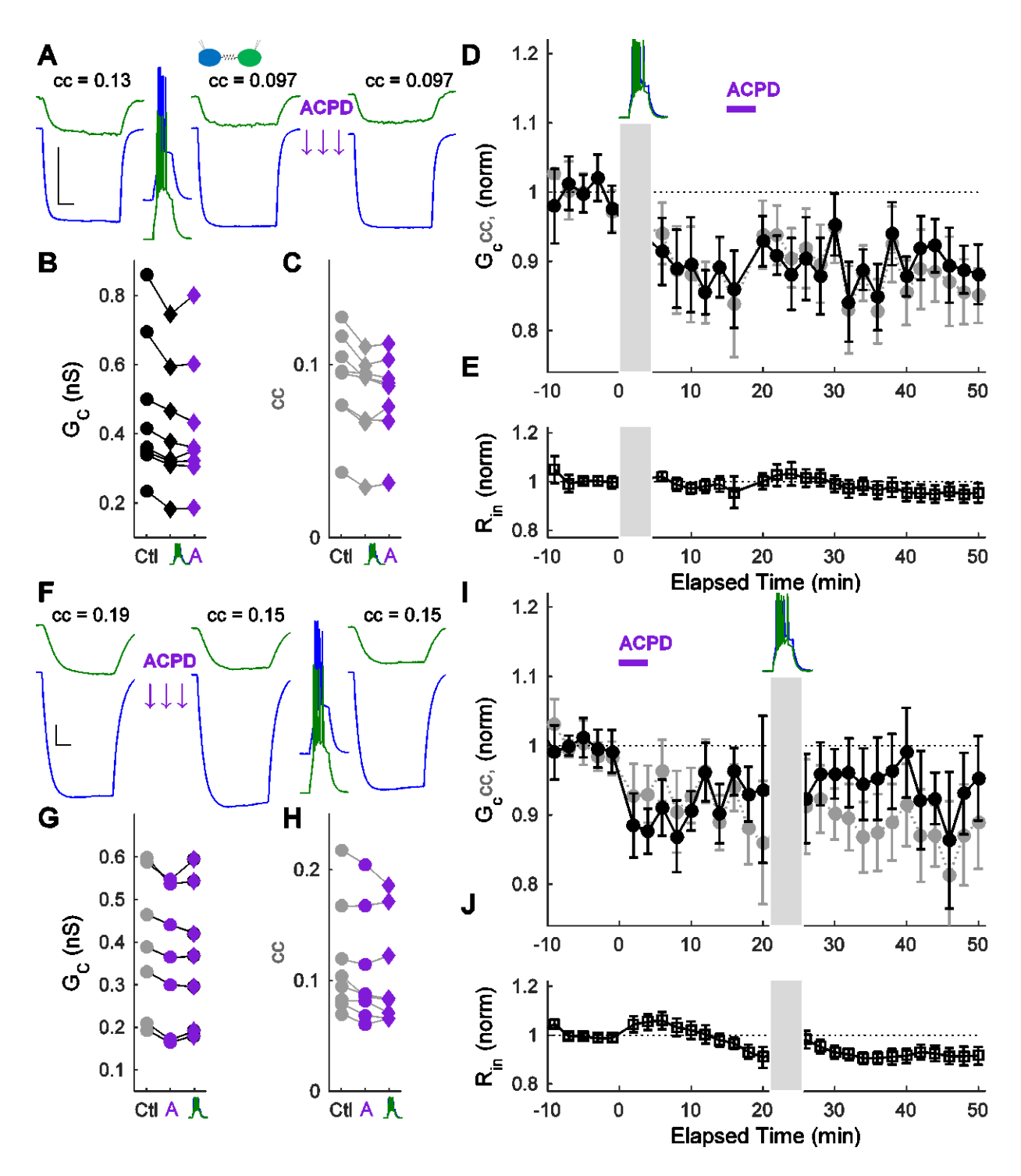


Figure 1. Paired bursting and ACPD each occlude further LTD induction. A) Example recordings from paired whole-cell recordings of electrically coupled neurons. In this pair, cc was initially 0.13. Scale bar 100 ms, 5 mV (blue), 1.67 mV (green). Following paired bursting in both cells, cc decreased to 0.097, and was unchanged after subsequent bath application of ACPD. B)

G_C and C) cc for the cohort of pairs used in this experiment, shown in control, after paired bursting (diamonds), and after subsequent ACPD application (purple). **D)** LTD was induced by paired bursting in two coupled TRN neurons. Between 0 and 15 min, ΔG_C (black) was -11.6 \pm 1.0%, $p_t = 0.003$, $p_s = 0.008$; and Δcc (grey) was -11.8 ± 1.3%, $p_t = 0.002$, $p_s = 0.008$ from prestimulus control (n = 8 pairs). ACPD was subsequently bath-applied for 4 min, resulting in no further changes in electrical synapse strength ($p_t = 0.58$, $p_s = 0.95$ for G_C , $p_t = 0.66$ and $p_s = 0.74$ for cc). E) Input resistance (R_{in}) over the experiment. F) In a pair with initial cc of 0.19, ACPD application decreased cc to 0.15 and was unchanged by subsequent paired bursting activity in both cells. Scale bar 100 ms, 5 mV (blue), 2.5 mV (green). G) G_C and H) cc for the cohort of pairs used in this experiment, shown in control, after ACPD application (purple), and after subsequent paired bursting (diamonds). I) LTD was induced by bath-applied ACPD (50 µM) in two coupled TRN neurons. Between 0 and 20 min, ΔG_C was -8.6 \pm 0.9%, p_t = 0.0001, p_s = 0.008; and Δcc was -8.2 ± 0.9%, p_t = 0.01, p_s = 0.02 from pre-stimulus control (n = 8 pairs). Paired bursting was then induced, resulting in no further changes in electrical synapse strength (p_t = 0.22, $p_s = 0.15$ for G_C , $p_t = 0.35$ and $p_s = 0.55$ for **cc** for the post-ACPD and post-burst comparisons). J) Input resistance (R_{in}) over the experiment.

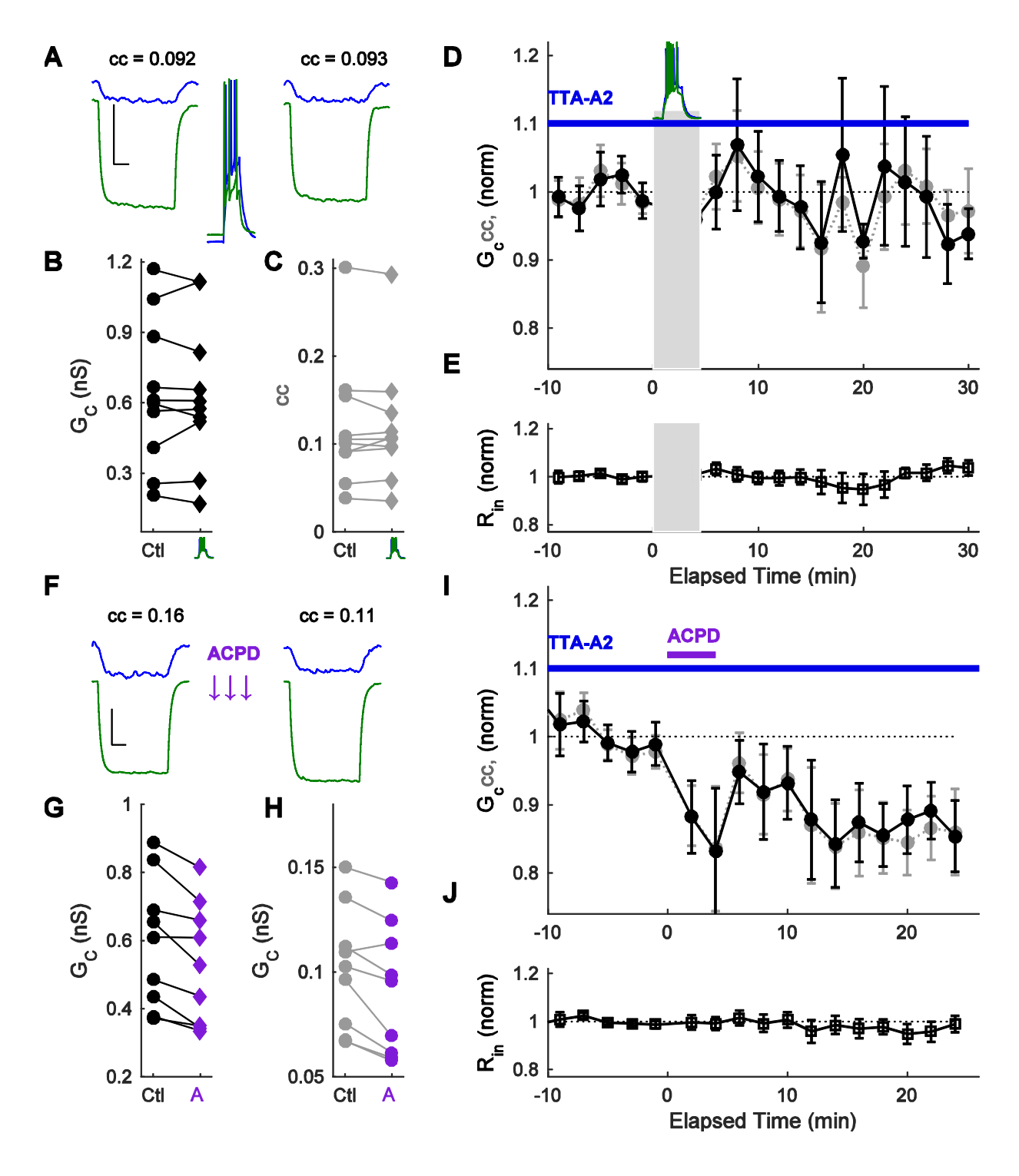


Figure 2. **T-type calcium channels are necessary for burst-induced but not ACPD-induced LTD. A)** Example recordings from a pair before and after paired bursting in TTA-A2. Scale bar 100 ms, 5 mV (green), 2.5 mV (blue). **B)** G_C and **C)** cc for the cohort of pairs used in this

experiment, shown in control and after paired bursting (diamonds). **D)** Paired bursting in two coupled TRN neurons did not result in LTD induction in the presence of the T-channel antagonist TTA-A2 ($\Delta G_C = -1.2 \pm 1.0\%$, $p_t = 0.9$, $p_s = 0.77$; $\Delta cc = -1.4 \pm 1.5\%$, p = 0.8, $p_s = 1$; $p_t = 10$ pairs). **E)** Input resistance ($p_t = 1.2 \pm 1.0\%$) over the experiment. **F)** Example recordings from a pair before and after ACPD application in TTA-A2. Scale bar 100 ms, 5 mV (green), 2.5 mV (blue). **G)** $p_t = 1.2 \pm 1.2 \pm$

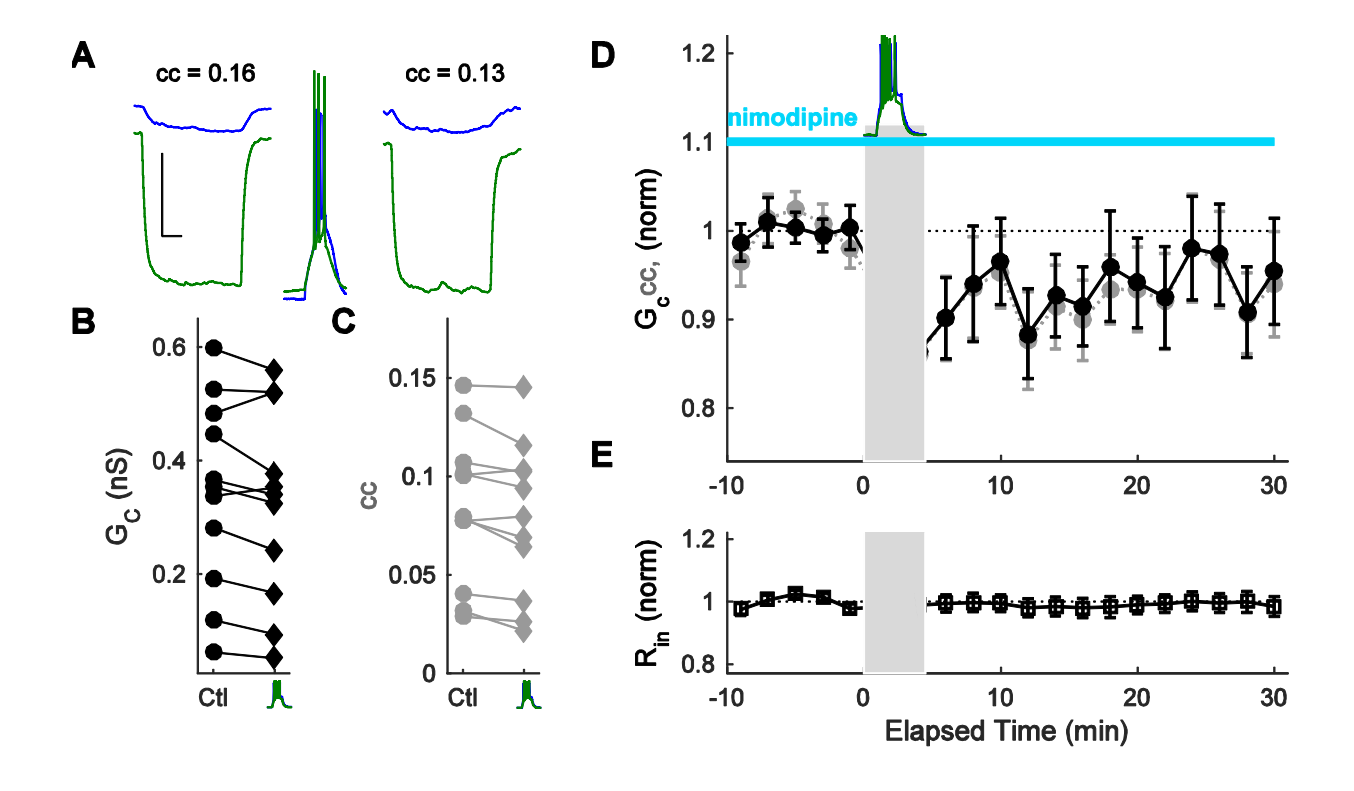


Figure 3. Calcium influx through high voltage-activated channels is necessary for burst-induced LTD. A) Example recordings from a pair before and after paired bursting in nimodipine. Scale bar 100 ms, 5 mV. B) G_C and C) cc for the cohort of pairs used in this

experiment, shown in control and after paired bursting (diamonds). **D)** Paired bursting induced decreased LTD in two coupled TRN neurons in the presence of the L-type channel antagonist nimodipine ($\Delta G_C = -6.2 \pm 0.8\%$, p = 0.047; $\Delta cc = -7.6 \pm 0.7\%$, p = 0.012; n = 11 pairs) **E)** Input resistance (R_{in}) over the experiment.

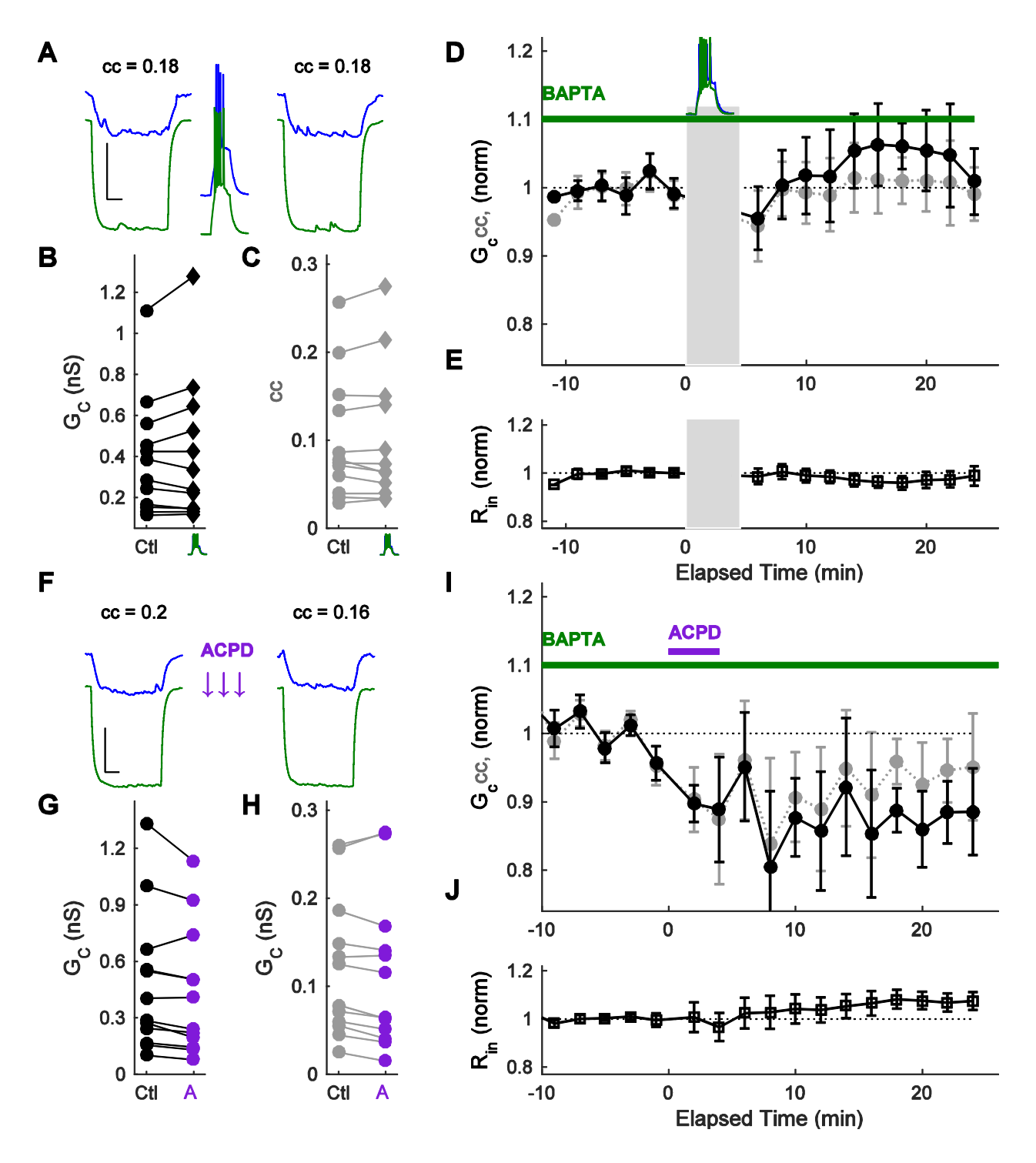


Figure 4. Calcium chelation prevents burst-induced but not ACPD-induced LTD. A)

Example recordings from a pair before and after paired bursting with BAPTA in the intracellular solution. Scale bar 100 ms, 5 mV (green), 2.5 mV (blue). **B)** G_C and **C)** cc for the cohort of pairs used in this experiment, shown in control and after paired bursting (diamonds). **D)** Paired

bursting failed to induce LTD in coupled TRN neurons, both with BAPTA chelating calcium in the intracellular solution. After paired bursting, $\Delta G_C = 1.67 \pm 1.2\%$, $p_t = 0.28$, $p_s = 0.47$ and $\Delta cc = -0.34 \pm 0.9\%$, $p_t = 0.71$, $p_s = 0.85$, n = 12 pairs) from control values. **E)** Input resistance (R_{in}) over the experiment. **F)** Example recordings from a pair before and after ACPD application with BAPTA. Scale bar 100 ms, 5 mV (green), 2.5 mV (blue). **G)** G_C and **H)** cc for the cohort of pairs used in this experiment, shown in control and after ACPD (purple). **I)** ACPD application induced LTD in coupled TRN neurons, both with BAPTA to chelate calcium in the intracellular solution. After paired bursting, ΔG_C was -12.0 \pm 1.2%, $p_t = 0.026$, $p_s = 0.015$ and $\Delta cc = -8.9 \pm 1.2\%$, $p_t = 4.4 \times 10^{-6}$, $p_s = 0.014$; n = 8 pairs) relative to control values. **J)** Input resistance (R_{in}) over the experiment.

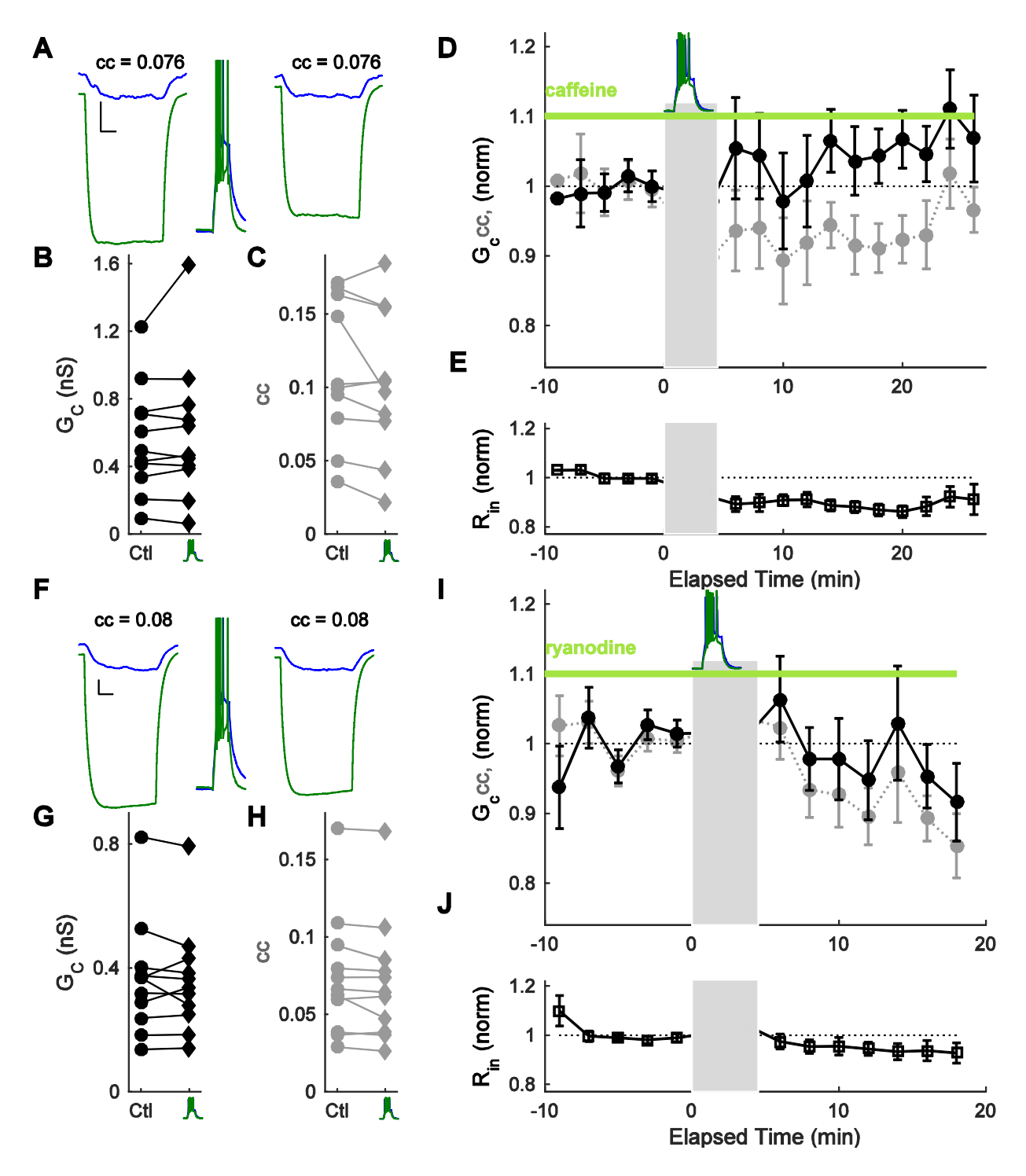


Figure 5. Ryanodine receptor-mediated intracellular calcium release is necessary for burst-induced LTD. A) Example recordings from a pair before and after paired bursting in caffeine. Scale bar 100 ms, 5 mV (green), 2.5 mV (blue). B) G_C and C) cc for the cohort of pairs used in this experiment, shown in control and after paired bursting (diamonds). D) Paired bursting was

induced in two coupled TRN neurons in the presence of the ryanodine receptor antagonist caffeine ($\Delta G_C = 6.7 \pm 1.4\%$, $p_t = 0.31$, $p_s = 0.41$; $\Delta R_{in} = -11.7 \pm 1.6\%$ p = 0.007; $\Delta cc = -5.7 \pm 1.0\%$, $p_t = 0.09$, $p_s = 0.31$; n = 11 pairs). **E)** Input resistance (R_{in}) over the experiment. **F)** Example recordings from a pair before and after paired bursting in ryanodine. Scale bar 100 ms, 5 mV (green), 2.5 mV (blue). **G)** G_C and **H)** cc for the cohort of pairs used in this experiment, shown in control and after paired bursting (diamonds). **I)** Paired bursting was induced in two coupled TRN neurons in the presence of the ryanodine receptor antagonist ryanodine (for t < 15 min, $\Delta G_C = 0.88 \pm 1.8\%$, $p_t = 0.6$, $p_s = 0.6$; $\Delta cc = -2.1 \pm 1.9\%$, $p_t = 0.07$, $p_s = 0.32$; n = 11 pairs). **F)** Input resistance (R_{in}) over the experiment.

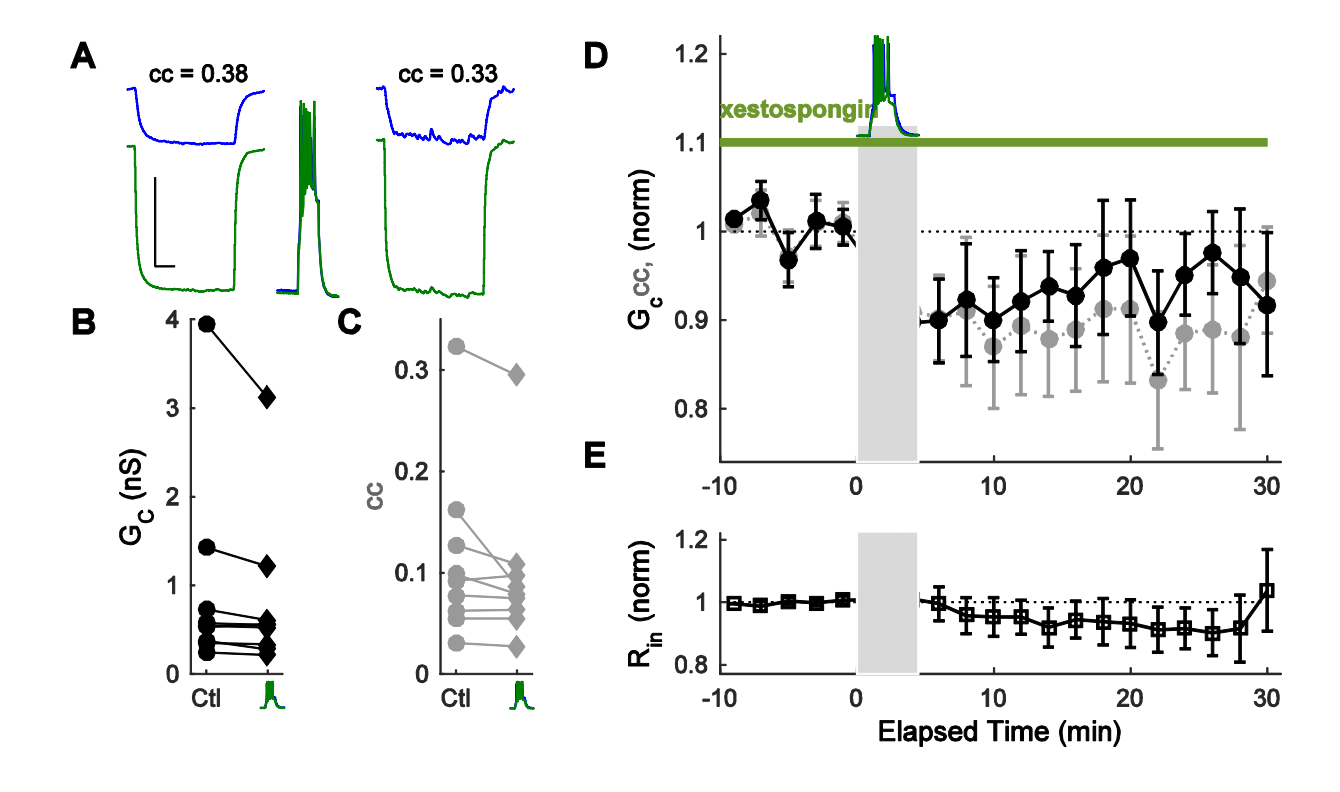


Figure 6. **IP**3-mediated intracellular calcium release is not necessary for burst-induced LTD **A**) Example recordings from a pair before and after paired bursting in xestospongin. Scale bar 100 ms, 5 mV. **B**) G_C and **C**) cc for the cohort of pairs used in this experiment, shown in control and after paired bursting (diamonds). **D**) Paired bursting was induced in two coupled TRN neurons in the presence of the IP₃ antagonist xestospongin ($\Delta G_C = -6.0 \pm 1.1\%$, $p_t = 0.16$, $p_s = 0.09$; $\Delta cc = -12.4 \pm 1.1\%$, $p_t = 0.093$, $p_s = 0.098$; n = 9 pairs). **E**) Input resistance (R_{in}) over the experiment.

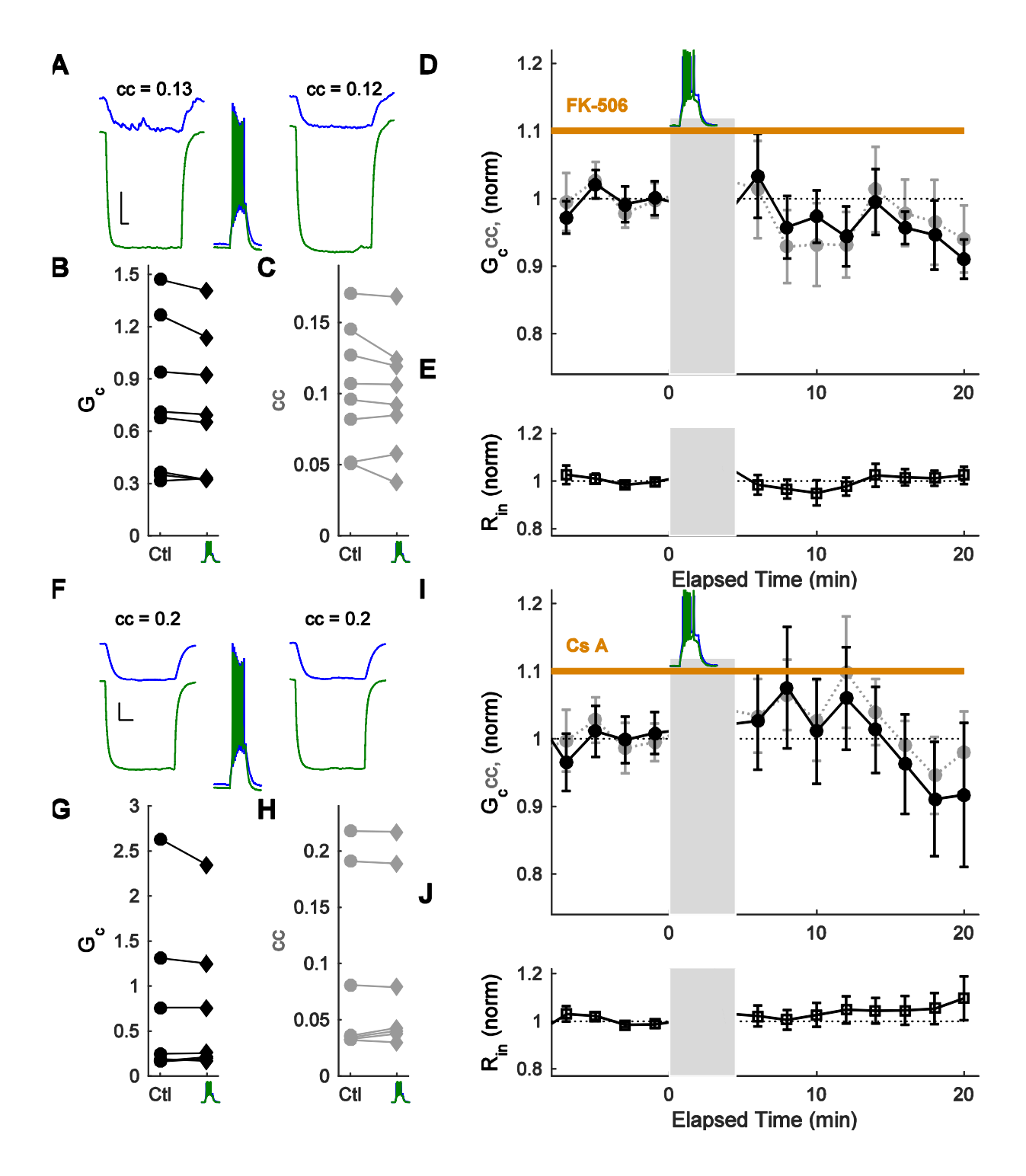


Figure 7. **Burst-induced LTD requires calcineurin activation. A)** Example recordings from a pair before and after paired bursting in FK-506. Scale bar 100 ms, 5 mV (green), 2.5 mV (blue). **B)** G_C and **C)** cc for the cohort of pairs used in this experiment, shown in control and after paired

bursting (diamonds). **D)** Paired bursting was induced in two coupled TRN neurons in the presence of the calcineurin antagonist FK-506, resulting in $\Delta G_C = -4.1 \pm 1.0\%$, $p_t = 0.91$, $p_s = 0.37$; $\Delta cc = -3.1 \pm 0.9\%$, $p_t = 0.28$, $p_s = 0.41$ relative to control values (n = 9 pairs). **E)** Input resistance (R_{in}) over the experiment. **F)** Example recordings from a pair before and after paired bursting with cyclosprin A in the internal solution. Scale bar 100 ms, 5 mV (green), 3 mV (blue). **G)** G_C and **H)** C_C for the cohort of pairs used in this experiment, shown in control and after paired bursting (diamonds). **I)** Paired bursting was induced in two coupled TRN neurons in the presence of the calcineurin inhibitor cyclosporin A ($\Delta G_C = 0.04 \pm 1.5\%$, $p_t = 0.36$, $p_s = 0.81$; $\Delta cc = -2.5 \pm 1.6\%$, $p_t = 0.38$, $p_s = 0.58$; n = 7 pairs). **F)** Input resistance (R_{in}) over the experiment.

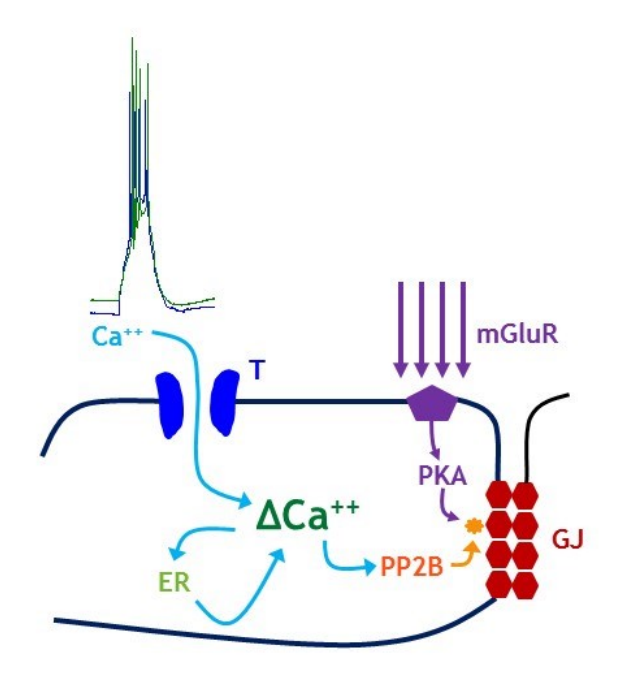


Figure 8. Proposed core mechanistic pathway for activity-dependent plasticity of electrical synapses. For paired bursting, calcium enters through voltage-gated channels (T). Influx of calcium causes calcium-induced calcium release from internal stores (ER), and activates calcineurin (PP2B), resulting in a dephosphorylation of the connexin36 protein (GJ). Separately, tetanic input activates metabotropic glutamate receptors (mGluR), and a chain eventually resuting in PKA activation also results in phosphorylation changes of the connexin36 protein (Wang et al., 2015).

References

- Alev C, Urschel S, Sonntag S, Zoidl G, Fort AG, Hoher T, Matsubara M, Willecke K, Spray DC & Dermietzel R. (2008). The neuronal connexin36 interacts with and is phosphorylated by CaMKII in a way similar to CaMKII interaction with glutamate receptors. *Proc Natl Acad Sci U S A* **105**, 20964-20969.
- Apostolides PF & Trussell LO. (2013). Regulation of interneuron excitability by gap junction coupling with principal cells. *Nat Neurosci* **16**, 1764-1772.
- Apostolides PF & Trussell LO. (2014). Control of Interneuron Firing by Subthreshold Synaptic Potentials in Principal Cells of the Dorsal Cochlear Nucleus. *Neuron*.
- Beierlein M, Gibson JR & Connors BW. (2003). Two dynamically distinct inhibitory networks in layer 4 of the neocortex. *J Neurophysiol* **90**, 2987-3000.
- Burr GS, Mitchell CK, Keflemariam YJ, Heidelberger R & O'Brien J. (2005). Calcium-dependent binding of calmodulin to neuronal gap junction proteins. *Biochem Biophys Res Commun* **335**, 1191-1198.
- Cachope R, Mackie K, Triller A, O'Brien J & Pereda AE. (2007). Potentiation of electrical and chemical synaptic transmission mediated by endocannabinoids. *Neuron* **56**, 1034-1047.
- Cachope R & Pereda AE. (2012). Two independent forms of activity-dependent potentiation regulate electrical transmission at mixed synapses on the Mauthner cell. *Brain Res*.
- Carter AG, Vogt KE, Foster KA & Regehr WG. (2002). Assessing the role of calcium-induced calcium release in short-term presynaptic plasticity at excitatory central synapses. *J Neurosci* **22**, 21-28.
- Chan GC, Tonegawa S & Storm DR. (2005). Hippocampal neurons express a calcineurin-activated adenylyl cyclase. *J Neurosci* **25**, 9913-9918.
- Collingridge GL, Peineau S, Howland JG & Wang YT. Long-term depression in the CNS. *Nat Rev Neurosci* **11**, 459-473.
- Coulon P, Herr D, Kanyshkova T, Meuth P, Budde T & Pape HC. (2009). Burst discharges in neurons of the thalamic reticular nucleus are shaped by calcium-induced calcium release. *Cell Calcium* **46,** 333-346.
- Crick F. (1984). Function of the thalamic reticular complex: the searchlight hypothesis. *Proc Natl Acad Sci U S A* **81**, 4586-4590.

- Curti S, Hoge G, Nagy JI & Pereda AE. (2012). Synergy between electrical coupling and membrane properties promotes strong synchronization of neurons of the mesencephalic trigeminal nucleus. *J Neurosci* **32**, 4341-4359.
- Curti S & Pereda AE. (2004). Voltage-dependent enhancement of electrical coupling by a subthreshold sodium current. *J Neurosci* **24,** 3999-4010.
- Del Corsso C, Iglesias R, Zoidl G, Dermietzel R & Spray DC. (2012). Calmodulin dependent protein kinase increases conductance at gap junctions formed by the neuronal gap junction protein connexin36. *Brain Res* **1487**, 69-77.
- Destexhe A. (1998). Spike-and-wave oscillations based on the properties of GABAB receptors. *J Neurosci* **18**, 9099-9111.
- Devor A & Yarom Y. (2002). Electrotonic coupling in the inferior olivary nucleus revealed by simultaneous double patch recordings. *J Neurophysiol* **87,** 3048-3058.
- Dudek SM & Bear MF. (1992). Homosynaptic long-term depression in area CA1 of hippocampus and effects of N-methyl-D-aspartate receptor blockade. *Proc Natl Acad Sci U S A* **89**, 4363-4367.
- Fortier PA. (2010). Detecting and estimating rectification of gap junction conductance based on simulations of dual-cell recordings from a pair and a network of coupled cells. *J Theor Biol* **265**, 104-114.
- Gafni J, Munsch JA, Lam TH, Catlin MC, Costa LG, Molinski TF & Pessah IN. (1997). Xestospongins: potent membrane permeable blockers of the inositol 1,4,5-trisphosphate receptor. *Neuron* **19**, 723-733.
- Galarreta M & Hestrin S. (2001). Electrical synapses between GABA-releasing interneurons. *Nat Rev Neurosci* **2**, 425-433.
- Gant JC, Blalock EM, Chen KC, Kadish I, Porter NM, Norris CM, Thibault O & Landfield PW. (2014). FK506-binding protein 1b/12.6: a key to aging-related hippocampal Ca2+ dysregulation? *Eur J Pharmacol* **739**, 74-82.
- Gibson JR, Beierlein M & Connors BW. (1999). Two networks of electrically coupled inhibitory neurons in neocortex. *Nature* **402**, 75-79.
- Haas JS. (2015). A new measure for the strength of electrical synapses. Front Cell Neurosci 9, 378.
- Haas JS & Landisman CE. (2012a). Bursts modify electrical synaptic strength. Brain Res.

- Haas JS & Landisman CE. (2012b). State-dependent modulation of gap junction signaling by the persistent sodium current. *Front Cell Neurosci* **5**, 31.
- Haas JS, Zavala B & Landisman CE. (2011). Activity-dependent long-term depression of electrical synapses. *Science* **334**, 389-393.
- Huguenard JR & Prince DA. (1992). A novel T-type current underlies prolonged Ca(2+)-dependent burst firing in GABAergic neurons of rat thalamic reticular nucleus. *J Neurosci* **12**, 3804-3817.
- Huguenard JR & Prince DA. (1994). Intrathalamic rhythmicity studied in vitro: nominal T-current modulation causes robust antioscillatory effects. *J Neurosci* **14**, 5485-5502.
- Inoue M, Duysens J, Vossen JM & Coenen AM. (1993). Thalamic multiple-unit activity underlying spikewave discharges in anesthetized rats. *Brain Res* **612**, 35-40.
- Kothmann WW, Li X, Burr GS & O'Brien J. (2007). Connexin 35/36 is phosphorylated at regulatory sites in the retina. *Vis Neurosci* **24**, 363-375.
- Kothmann WW, Trexler EB, Whitaker CM, Li W, Massey SC & O'Brien J. (2012). Nonsynaptic NMDA receptors mediate activity-dependent plasticity of gap junctional coupling in the All amacrine cell network. *J Neurosci* **32**, 6747-6759.
- Kraus RL, Li Y, Gregan Y, Gotter AL, Uebele VN, Fox SV, Doran SM, Barrow JC, Yang ZQ, Reger TS, Koblan KS & Renger JJ. (2010). In vitro characterization of T-type calcium channel antagonist TTA-A2 and in vivo effects on arousal in mice. *J Pharmacol Exp Ther* **335**, 409-417.
- Landisman CE & Connors BW. (2005). Long-term modulation of electrical synapses in the mammalian thalamus. *Science* **310**, 1809-1813.
- Landisman CE, Long MA, Beierlein M, Deans MR, Paul DL & Connors BW. (2002). Electrical synapses in the thalamic reticular nucleus. *J Neurosci* **22**, 1002-1009.
- Li Y, Wu LJ, Legendre P & Xu TL. (2003). Asymmetric cross-inhibition between GABAA and glycine receptors in rat spinal dorsal horn neurons. *J Biol Chem* **278**, 38637-38645.
- Liu J, Farmer JD, Jr., Lane WS, Friedman J, Weissman I & Schreiber SL. (1991). Calcineurin is a common target of cyclophilin-cyclosporin A and FKBP-FK506 complexes. *Cell* **66**, 807-815.
- Long MA, Deans MR, Paul DL & Connors BW. (2002). Rhythmicity without synchrony in the electrically uncoupled inferior olive. *J Neurosci* **22**, 10898-10905.

- Long MA, Landisman CE & Connors BW. (2004). Small clusters of electrically coupled neurons generate synchronous rhythms in the thalamic reticular nucleus. *J Neurosci* **24**, 341-349.
- Malenka RC & Bear MF. (2004). LTP and LTD: an embarrassment of riches. Neuron 44, 5-21.
- Mann-Metzer P & Yarom Y. (1999). Electrotonic coupling interacts with intrinsic properties to generate synchronized activity in cerebellar networks of inhibitory interneurons. *J Neurosci* **19**, 3298-3306.
- Mathy A, Clark BA & Hausser M. (2014). Synaptically induced long-term modulation of electrical coupling in the inferior olive. *Neuron* **81,** 1290-1296.
- McAlonan K, Cavanaugh J & Wurtz RH. (2006). Attentional modulation of thalamic reticular neurons. *J Neurosci* **26**, 4444-4450.
- Mitropoulou G & Bruzzone R. (2003). Modulation of perch connexin35 hemi-channels by cyclic AMP requires a protein kinase A phosphorylation site. *J Neurosci Res* **72**, 147-157.
- Neyer C, Herr D, Kohmann D, Budde T, Pape HC & Coulon P. (2016). mGluR-mediated calcium signalling in the thalamic reticular nucleus. *Cell Calcium* **59**, 312-323.
- Ohara PT & Lieberman AR. (1985). The thalamic reticular nucleus of the adult rat: experimental anatomical studies. *J Neurocytol* **14**, 365-411.
- Pereda AE, Bell TD, Chang BH, Czernik AJ, Nairn AC, Soderling TR & Faber DS. (1998). Ca2+/calmodulin-dependent kinase II mediates simultaneous enhancement of gap-junctional conductance and glutamatergic transmission. *Proc Natl Acad Sci U S A* **95**, 13272-13277.
- Pereda AE & Faber DS. (1996). Activity-dependent short-term enhancement of intercellular coupling. *J Neurosci* **16**, 983-992.
- Pinault D & Deschenes M. (1998). Projection and innervation patterns of individual thalamic reticular axons in the thalamus of the adult rat: a three-dimensional, graphic, and morphometric analysis. *J Comp Neurol* **391**, 180-203.
- Sevetson J & Haas JS. (2015). Asymmetry and modulation of spike timing in electrically coupled neurons. *J Neurophysiol*, jn 00843 02014.
- Steriade M. (2005). Sleep, epilepsy and thalamic reticular inhibitory neurons. *Trends Neurosci* **28,** 317-324.

- Steriade M, Domich L, Oakson G & Deschenes M. (1987). The deafferented reticular thalamic nucleus generates spindle rhythmicity. *J Neurophysiol* **57**, 260-273.
- Svoboda K & Mainen ZF. (1999). Synaptic [Ca2+]: intracellular stores spill their guts. Neuron 22, 427-430.
- Talley EM, Cribbs LL, Lee JH, Daud A, Perez-Reyes E & Bayliss DA. (1999). Differential distribution of three members of a gene family encoding low voltage-activated (T-type) calcium channels. *J Neurosci* **19**, 1895-1911.
- Turecek J, Yuen GS, Han VZ, Zeng XH, Bayer KU & Welsh JP. (2014). NMDA receptor activation strengthens weak electrical coupling in mammalian brain. *Neuron* **81**, 1375-1388.
- von Krosigk M, Bal T & McCormick DA. (1993). Cellular mechanisms of a synchronized oscillation in the thalamus. *Science* **261**, 361-364.
- Wang Z, Neely R & Landisman CE. (2015). Activation of Group I and Group II Metabotropic Glutamate Receptors Causes LTD and LTP of Electrical Synapses in the Rat Thalamic Reticular Nucleus. *J Neurosci* **35**, 7616-7625.
- Xia Z & Storm DR. (2005). The role of calmodulin as a signal integrator for synaptic plasticity. *Nat Rev Neurosci* **6**, 267-276.
- Yang XD, Korn H & Faber DS. (1990). Long-term potentiation of electrotonic coupling at mixed synapses. *Nature* **348**, 542-545.